LASER INTERFEROMETER GRAVITATIONAL WAVE OBSERVATORY
- LIGO -
CALIFORNIA INSTITUTE OF TECHNOLOGY
MASSACHUSETTS INSTITUTE OF TECHNOLOGY

2023/09/04

FINAL REPORT

Sophia Adams

California Institute of Technology
LIGO Project, MS 18-34
Pasadena, CA 91125
Phone (626) 395-2129
Fax (626) 304-9834
E-mail: info@ligo.caltech.edu

Massachusetts Institute of Technology
LIGO Project, Room NW22-295
Cambridge, MA 02139
Phone (617) 253-4824
Fax (617) 253-7014
E-mail: info@ligo.mit.edu

LIGO Hanford Observatory
Route 10, Mile Marker 2
Richland, WA 99352
Phone (509) 372-8106
Fax (509) 372-8137
E-mail: info@ligo.caltech.edu

LIGO Livingston Observatory
19100 LIGO Lane
Livingston, LA 70754
Phone (225) 686-3100
Fax (225) 686-7189
E-mail: info@ligo.caltech.edu

http://www.ligo.caltech.edu/

Quality Testing Optically Contacted Bonds

Sophia Adams, Caltech

Mentor: Professor Rana Adhikari, Caltech

Abstract

Optical contacting is a type of bonding that can be achieved when flat, polished surfaces are brought into close contact. When used as a replacement for fused silica, optically contacted silicon has the potential to increase the sensitivity of LIGO Voyager to gravitational waves. This project is aimed at determining the quality factor of optically contacted silicon bonds in order to quantify their potential to reduce the noise in LIGO Voyager. By maximizing the energy contribution from the bond and oscillating a silicon cantilever, the quality factor of the bond can be estimated. The bond energy was found to be highest when using a rectangular cantilever with a 1.03 cm length, .5 mm width, and .1 mm height.

1 Introduction

1.1 Background

Optical contacting uses intermolecular forces like the Van der Waals dispersion force to bond surfaces without glue. Optical contacting works by reducing the space between molecules of different surfaces. In order to reduce the space between molecules, the surfaces must be very flat and polished. Any diversity in the geometry of the plates would decrease the strength of the bond [1]. Once the surfaces are made flat and polished, they can be brought together, and the strength of the intermolecular forces will increase and join the two surfaces into one. Though heat and pressure are known to increase the strength of the bond, little research has gone into characterizing optically contacted bonds [2].

1.2 Motivation

Optical contacting bonding has important implications for space equipment. Equipment in space relies on the presence of strong, light bonds. Adhesives may sometimes outgas and produce contaminants. Optical contacting bonds do not outgas and so could be one solution to the contaminant problem. Optical contacting bonds could also reduce the risk of failing that comes with having adhesives with different chemical and thermal properties. Optical contacting bonding is particularly useful in high sensitivity probes such as LISA and the LIGO Voyager when it is used to bond silicon, which has a small thermal expansion coefficient [3]. The ultimate goal is to use optical contacting in the LIGO Voyager to improve its sensitivity to gravitatonal waves.

2 Experimental Setup

This project focuses on testing the mechanical loss of an optically contacted bond within a silicon wafer. The silicon wafer cantilever will be given an initial impulse, and the ring-down will be measured. The quality factor (the inverse of the mechanical loss) can be obtained from a measure of how damped the response is. In order to measure the oscillations of the cantilever, an optical lever was setup as in Figure 1.

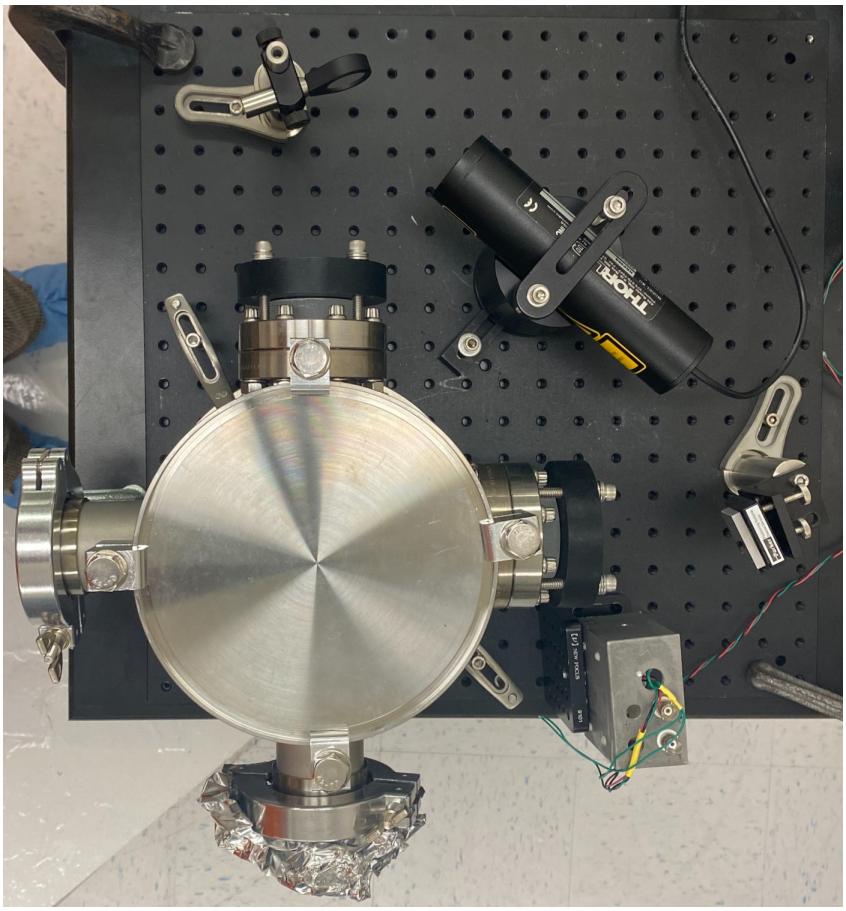

Figure 1: Experimental setup for measurement of ring-down. Notice the laser beam hits a mirror and is then directed into a vacuum chamber containing a silicon rectangular cantilever which is clamped. The beam then hits another mirror and is directed into a photo diode connected to a power supply and a Moku which acts as an oscilloscope.

The top of the vacuum chamber was knocked on, oscillating the clamped cantilever. The subsequent ring-down of the laser was measured by the a diode.

3 Cantilever Geometry

In order to make the measurement of the quality factor of the bond precise, the energy in the bond should be maximized while the energy in the rest of the system (the silicon and

the clamp) should be minimized, as described by Figure 3 (derived from Figure 2). An appropriate geometry should be selected for this purpose.

$$\frac{1}{Q_{system}} = \sum_{i=1}^{n} \frac{E_i}{E_{system}} \frac{1}{Q_i}$$

Figure 2: Equation for the quality factor of a system made up of n different materials.

$$\frac{1}{Q_{system}} = \frac{E_{silicon}}{E_{system}} \frac{1}{Q_{silicon}} + \frac{E_{bond}}{E_{system}} \frac{1}{Q_{bond}}$$

Figure 3: Equation for the quality factor of the optically contacted silicon considering the solid silicon and bond to be different materials.

Gentle nodal suspension is an experimentally tested way of measuring the quality factor of a substrate [4]. However, gentle nodal suspension fails at cryogenic temperatures, which have been shown to yield high Q measurements [5].

Three different cantilever geometries were analyzed in order to find a suitable energy ratio between the bond and the rest of the silicon wafer. The ratio between shear and bending energy was estimated for the geometries shown in Figure 4 using the following equations where M is the moment, I is the moment of inertia, l is the length, E is young's modulus, K is a constant that depends on the geometry (1.11 for circular and 0.5 for rectangular sections), V is the traverse shear force, G is the modulus of rigidity, and A is the cross sectional area.

$constant\ bending\ energy = \frac{M^2 l}{2EI}$

$constant\ traverse\ shear\ energy = \frac{KV^2 l}{2GA}$

A tapered cantilever was selected to maximize shear stress and minimize bending. In a tapered cantilever, the bond in the middle will experience maximum shear stress, and the whole cantilever will have its bending stress minimized. However in general, the bending stress in a cantilever is greater than the shear stress. The actual ratio was determined using finite element analysis in COMSOL. The results are presented in the following sections.

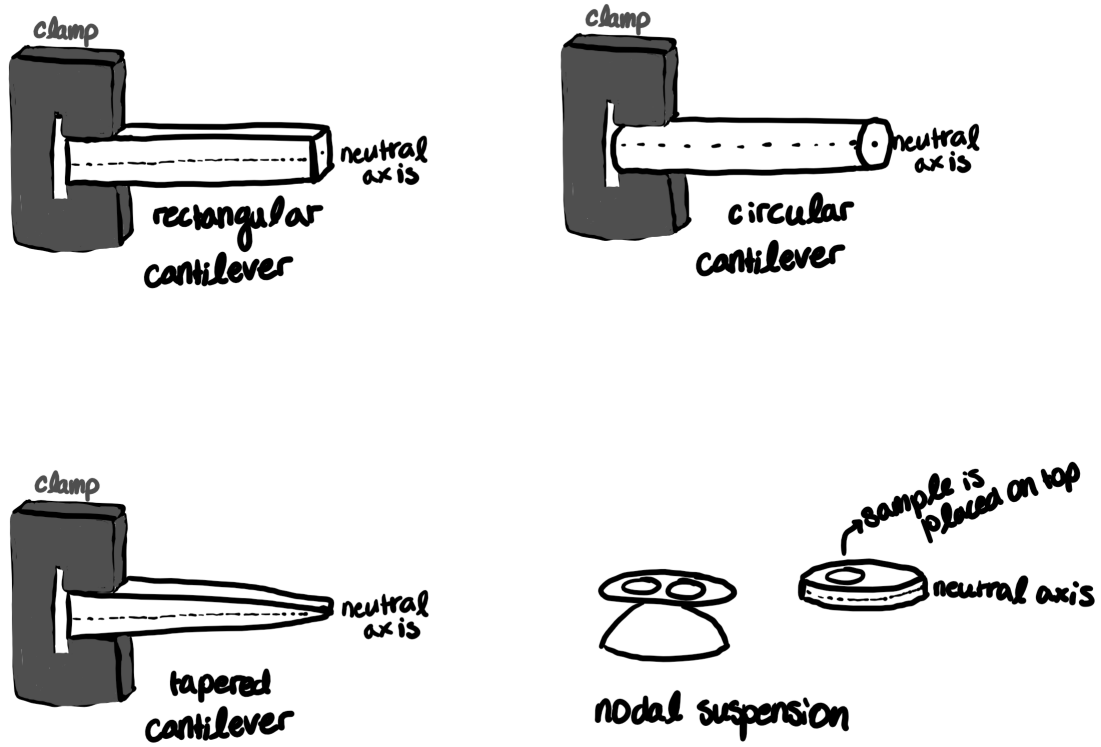

Figure 4: A diagram of three sample cantilever geometries and the setup for gentle nodal suspension.

3.1 Pizza Cantilever

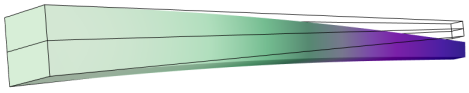

Figure 5: Stresses on a pizza cantilever at 34557 Hz.

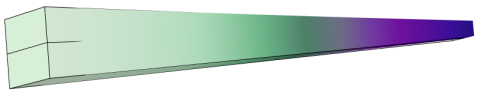

Figure 6: Stresses on a pizza cantilever at 51994 Hz.

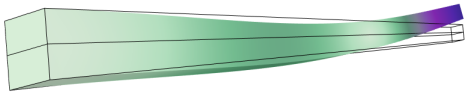

Figure 7: Stresses on a pizza cantilever at 1.0385E5 Hz.

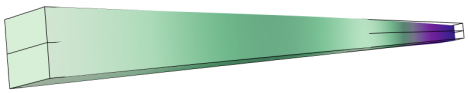

Figure 8: Stresses on a pizza cantilever at 1.5129E5 Hz.

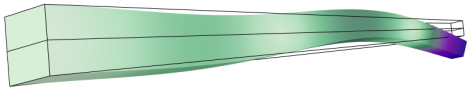

Figure 9: Stresses on a pizza cantilever at 2.1981E5 Hz.

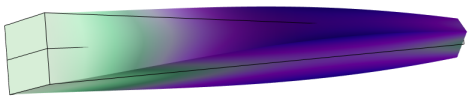

Figure 10: Stresses on a pizza cantilever at 2.7240E5 Hz.

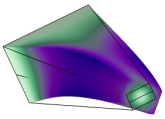

Figure 11: Stresses on a pizza cantilever at 2.7240E5 Hz viewed from the front. Note that this view is shown because the stresses are nonuniform through the center. All other eigenfrequencies have uniform stresses through their middle.

Table 1: Pizza Cantilever Energies.

Eigenfrequency (Hz)	**Bulk (N*m)**	**Shear (N*m)**	**Total (J)**	**Shear/Bulk**
34557	6.0-13	2.5E-12	1.5E-12	4.2
51994	1.4E-12	5.8E-12	3.6E-12	4.3
1.0385E5	2.8E-12	1.2E-11	7.4E-12	4.3
1.5129E5	5.8E-12	2.8E-11	1.7E-11	4.8
2.1981E5	1.0E-11	4.7E-11	2.8E-11	4.6
2.7240E5	2.1E-12	5.6E-10	2.8E-10	270

3.2 Rectangular Cantilever

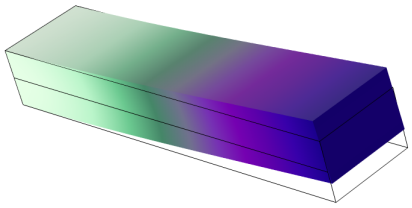

Figure 12: Stresses on a rectangular cantilever at 20385 Hz.

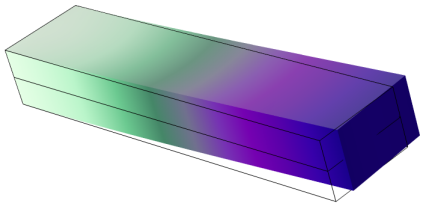

Figure 13: Stresses on a rectangular cantilever at 30507 Hz.

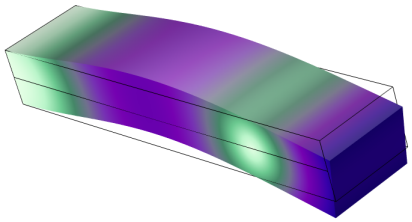

Figure 14: Stresses on a rectangular cantilever at 1.1796E5 Hz.

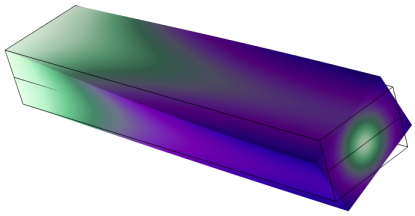

Figure 15: Stresses on a rectangular cantilever at 1.2326E5 Hz.

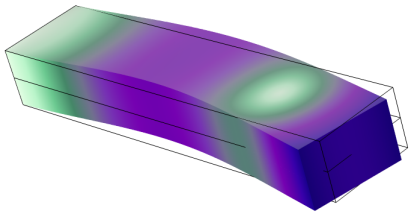

Figure 16: Stresses on a rectangular cantilever at 1.6250E5 Hz.

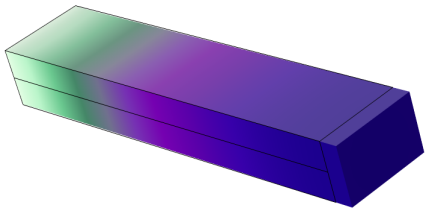

Figure 17: Stresses on a rectangular cantilever at 2.2601E5 Hz.

Table 2: Rectangular Cantilever Energies.

Eigenfrequency (Hz)	**Bulk (N*m)**	**Shear (N*m)**	**Total (J)**	**Shear/Bulk**
20385	2.2E-12	8.6E-12	5.4E-12	3.9
30507	4.8E-12	2.0E-11	1.2E-11	4.2
1.1796E5	7.3E-11	3.3E-10	2.0E-10	4.5
1.2326E5	1.4E-12	3.6E-10	1.8E-10	260
1.6250E5	1.3E-10	7.3E-10	4.3E-10	5.4
2.2601E5	5.1E-10	2.1E-9	1.3E-9	4.1

3.3 Geometry Selection

For both geometries, the highest shear to bulk energy ratio was at an eigenfrequency which caused the cantilever to twist. However, looking at the graphs (figure 15 and Figure 11), the highest energy contribution was from the outside edges. This eigenfrequency was therefore not considered when selecting the best ratio. The next highest overall ratio was the rectangular cantilever at 1.6250E5 Hz, and the ratio was 5.420. The highest energy contribution was from the tip and the middle section. The rectangular cantilever was selected for this reason.

3.4 Rectangular Cantilever With Lab Dimensions

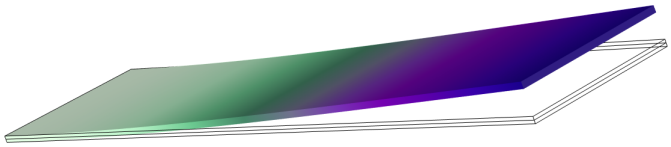

Figure 18: Stresses on a rectangular cantilever at 1266 Hz.

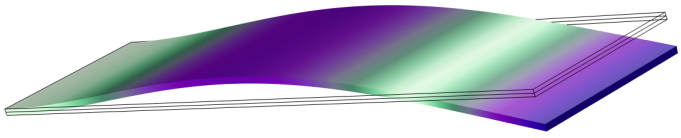

Figure 19: Stresses on a rectangular cantilever at 7927.1 Hz.

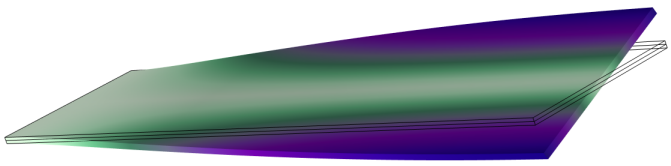

Figure 20: Stresses on a rectangular cantilever at 12012 Hz.

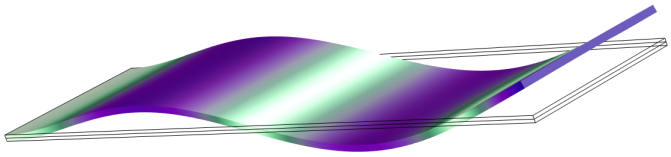

Figure 21: Stresses on a rectangular cantilever at 22212 Hz.

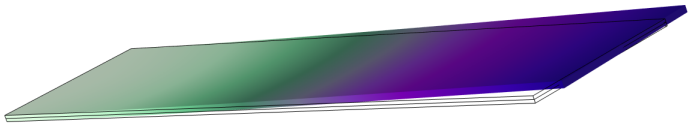

Figure 22: Stresses on a rectangular cantilever at 30433 Hz.

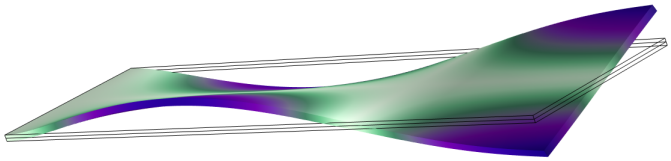

Figure 23: Stresses on a rectangular cantilever at 36767 Hz.

Table 3: Rectangular Cantilever With Lab Dimensions Energies.

Eigenfrequency (Hz)	**Bulk (N*m)**	**Shear (N*m)**	**Total (J)**	**Shear/Bulk**
1266.0	5.3E-16	1.9E-15	1.2E-15	3.6
7927.1	2.0E-14	7.6E-14	4.8E-14	3.7
12012	2.3E-15	1.4E-13	6.9E-14	58
22212	1.6E-13	5.8E-13	3.7E-13	3.6
30433	2.7E-13	1.2E-12	7.4E-13	4.5
36767	3.6E-14	1.2E-12	6.0-13	3.3

3.5 Discussion on the Dimensions

The thinner the cantilever, the more vertical bending there is and the smaller the shear to bulk ratio. A pizza cantilever with the same dimensions as a rectangular cantilever at its base would thin out near the end and have a smaller shear to bulk ratio overall (Table 4).

Table 4: Pizza Cantilever With Lab Dimensions Energies.

Eigenfrequency (Hz)	**Bulk (N*m)**	**Shear (N*m)**	**Total (J)**	**Shear/Bulk**
2085.9	1.5E-16	5.9E-16	3.7E-16	4.0
6624.0	8.0E-16	3.2E-15	2.0E-15	4.0
14820	3.4E-15	1.3E-14	8.2E-15	3.9
25628	2.6E-15	1.9E-13	9.9E-14	75
26899	1.1E-14	4.0E-14	2.5E-14	3.8
42943	2.6E-14	9.8E-14	6.2E-14	3.7

3.6 Dimension Optimization

An analysis of the shear/bulk energy ratio and (inner surface energy)/(total energy) ratio was completed over a range of different lengths and widths in order to determine the optimal dimensions (Figures 25, 26, 27, 28, and 29). A boundary load was added and a stationary study was run in order to better visualize the results (Figure 30). Fminsearch was used in order to find a minimum ratio of total energy to inner surface energy starting with a 1 cm length, .5 mm width, and .3 mm height. The ideal dimensions were found to be 1.03 cm for the length, .5 mm for the width, and .1 mm for the height. The energy in the bond was found to be highest when the cantilever was oscillated at an eigenfrequency which pulled on the beam normal to the clamped end (in the z direction in Figure 24).

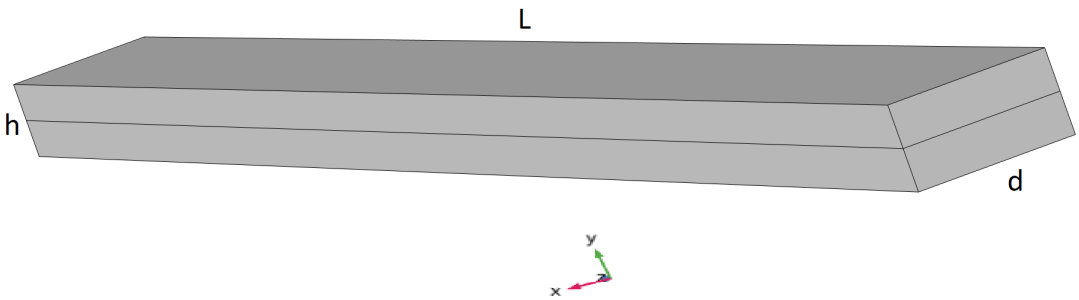

Figure 24: Drawing of a rectangular cantilever with the width (d), height (h), and length (L) labelled.

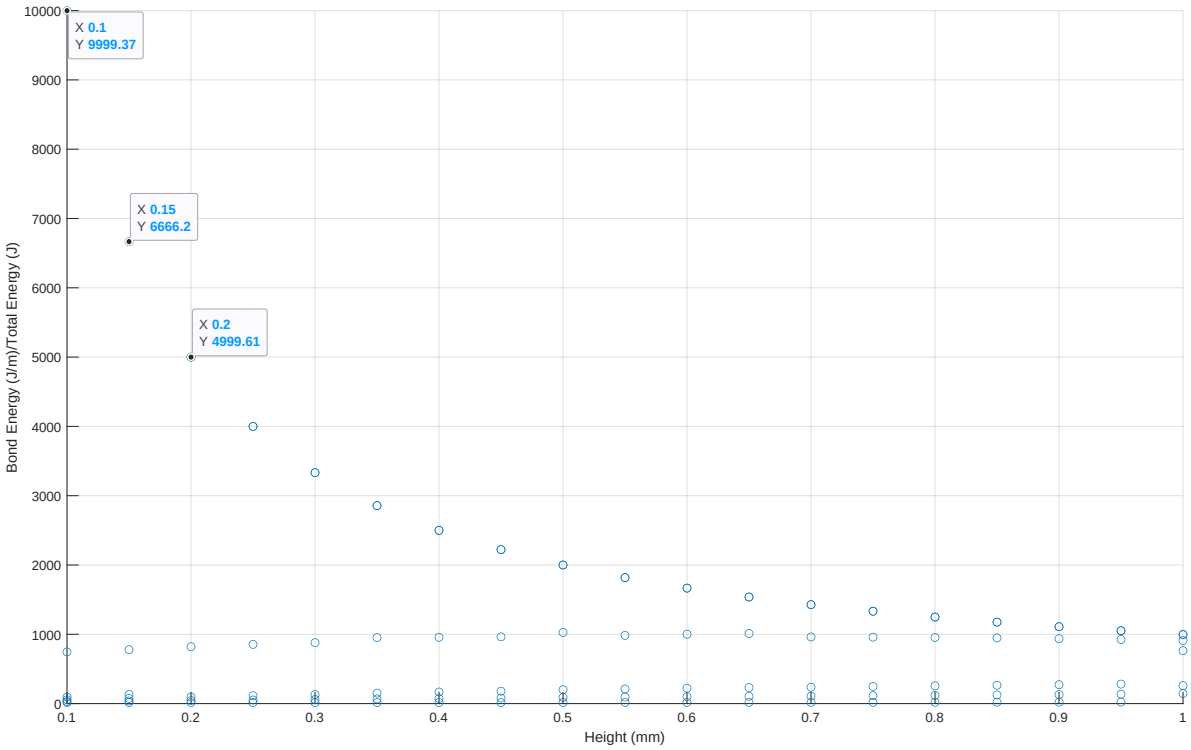

Figure 25: Graph showing how the bond/total energy ratio changes with the height from 0.1 mm to 1 mm. Each point is associated with a different eigenfrequency. Six different eigenfrequencies are plotted for each set of parameters.

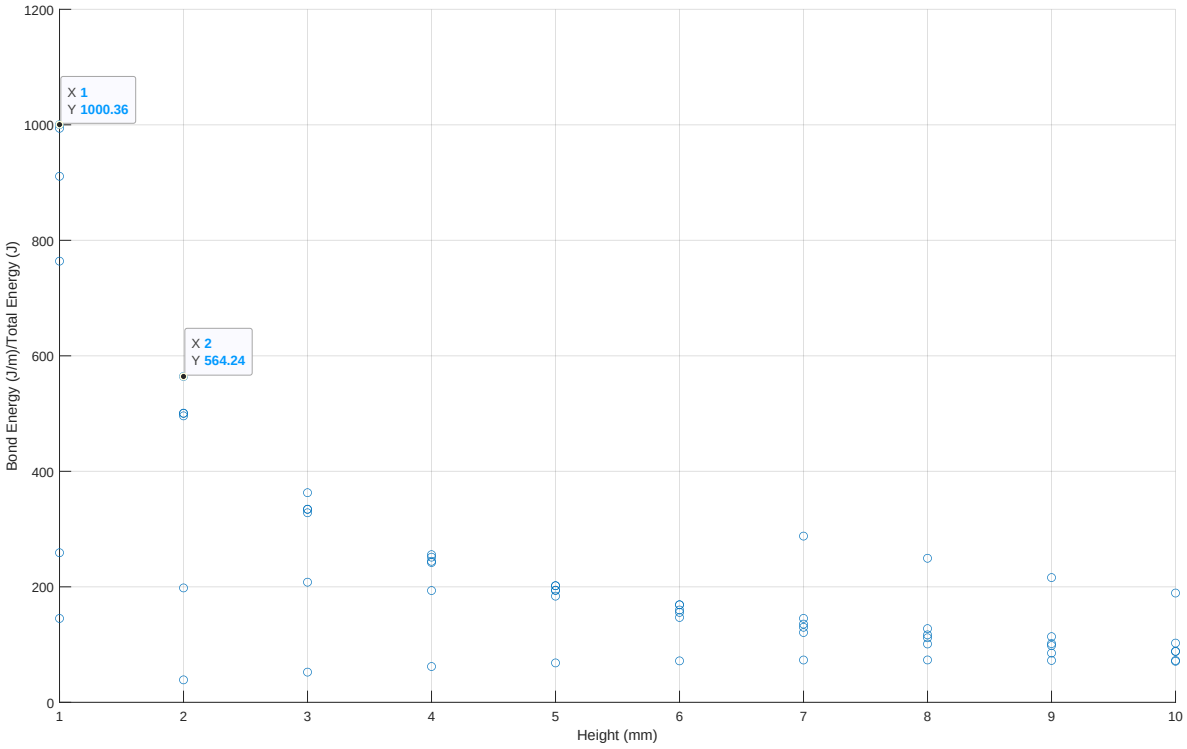

Figure 26: Graph showing how the bond/total energy ratio changes with the height from 1 mm to 10 mm. Each point is associated with a different eigenfrequency. Six different eigenfrequencies are plotted for each set of parameters.

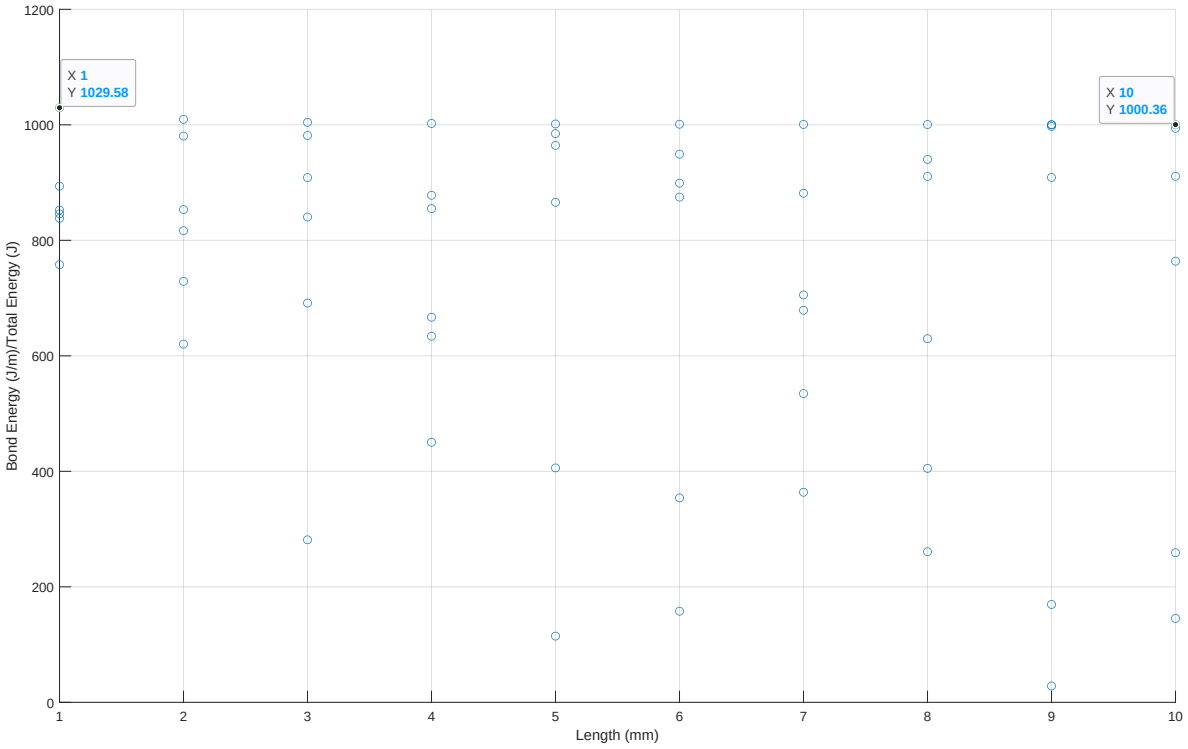

Figure 27: Graph showing how the bond/total energy ratio changes with the length from 1 mm to 10 mm. Each point is associated with a different eigenfrequency. Six different eigenfrequencies are plotted for each set of parameters.

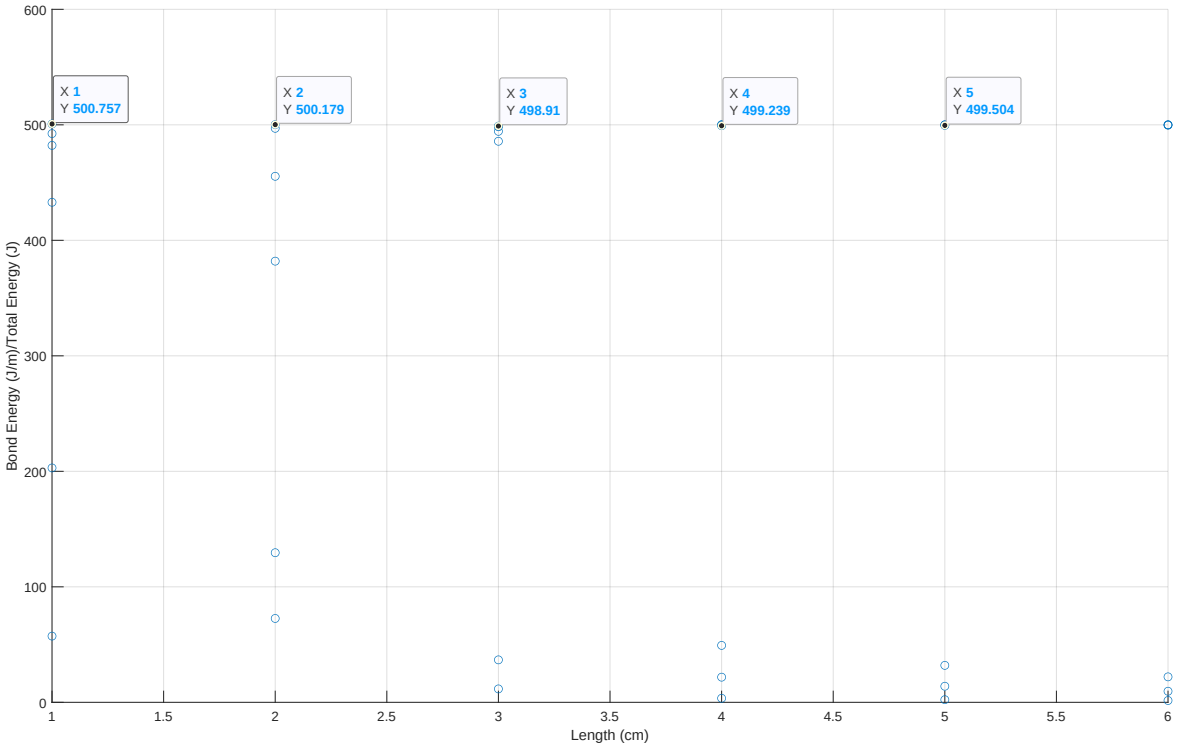

Figure 28: Graph showing how the bond/total energy ratio changes with the length from 1 cm to 6 cm. Each point is associated with a different eigenfrequency. Six different eigenfrequencies are plotted for each set of parameters.

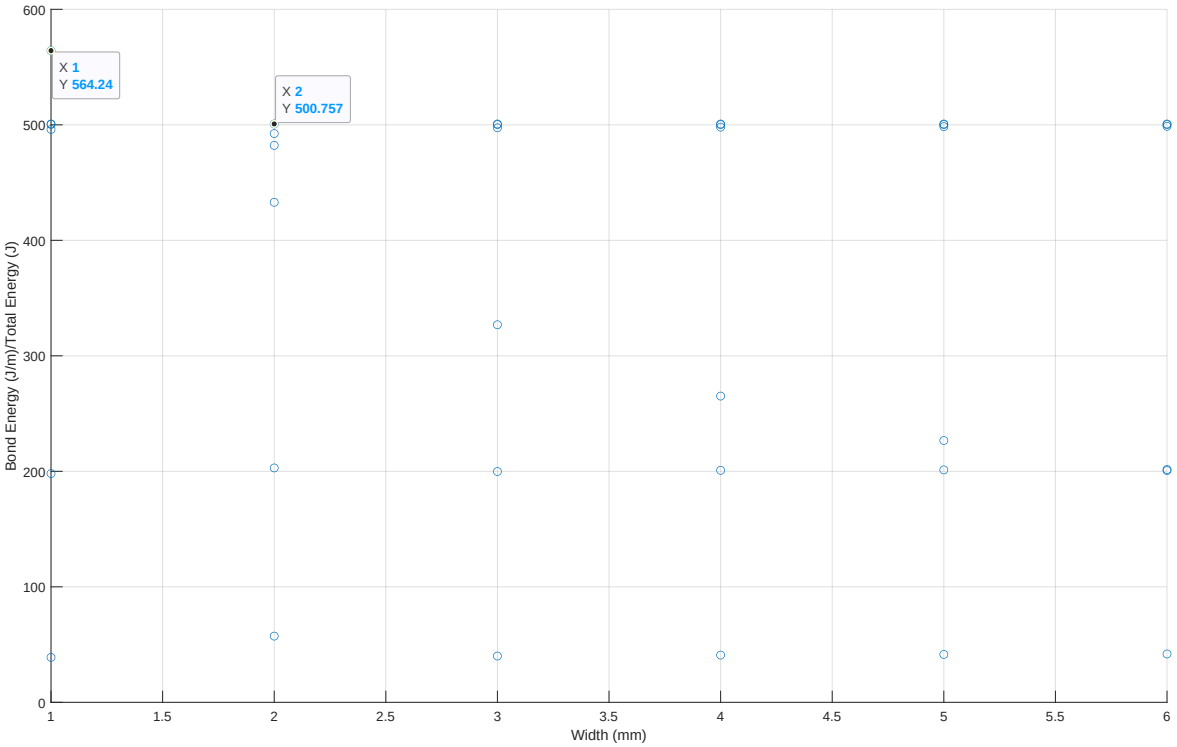

Figure 29: Graph showing how the bond/total energy ratio changes with the width from 1 mm to 6 mm. Each point is associated with a different eigenfrequency. Six different eigenfrequencies are plotted for each set of parameters.

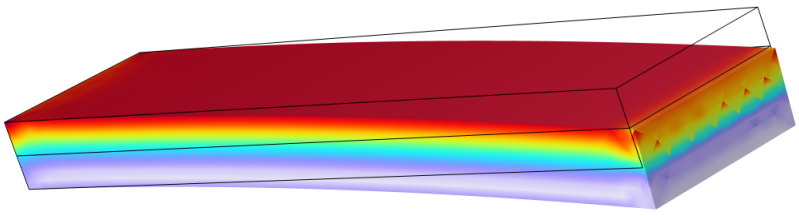

Figure 30: Plot of von Mises stress for a cantilever with a boundary load. Red/darker areas correspond to more stress.

4 Parameter Estimation

An initial test of the experimental setup was conducted by gently knocking on the top of the vacuum chamber. The oscillation of the laser was measured on a Moku (Figure 31), and the following analysis was performed to find the quality factor.

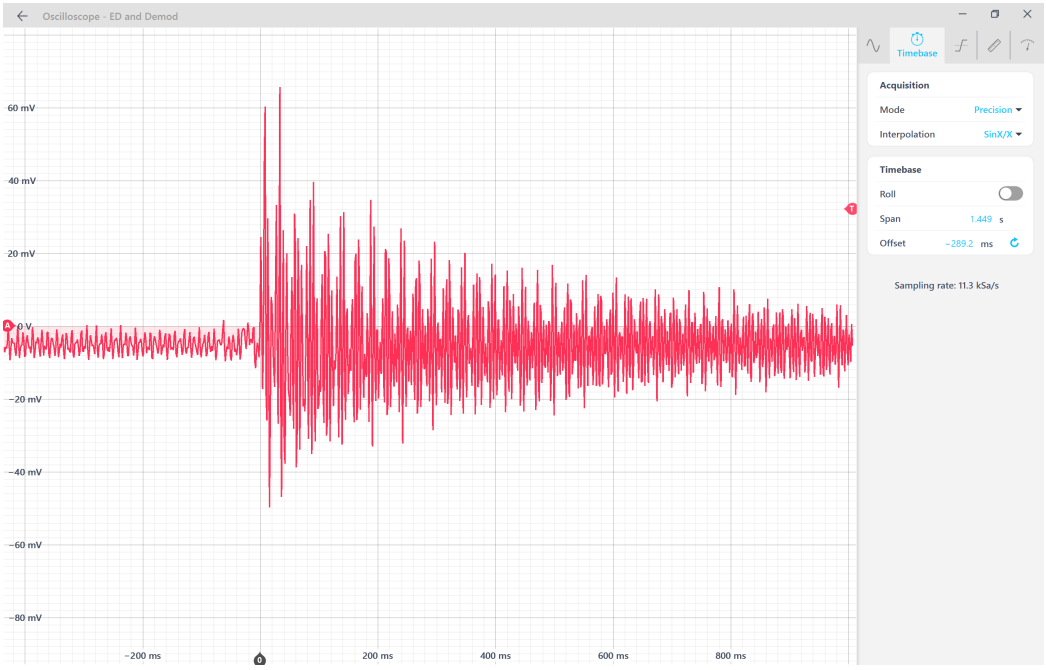

Figure 31: Screenshot of the laser signal measured on the Moku.

The signal was modeled in python using the scipy curve fit function and the following equation.

$$y = Ae^{w_1 t} \sin(w_2 t + \phi)$$

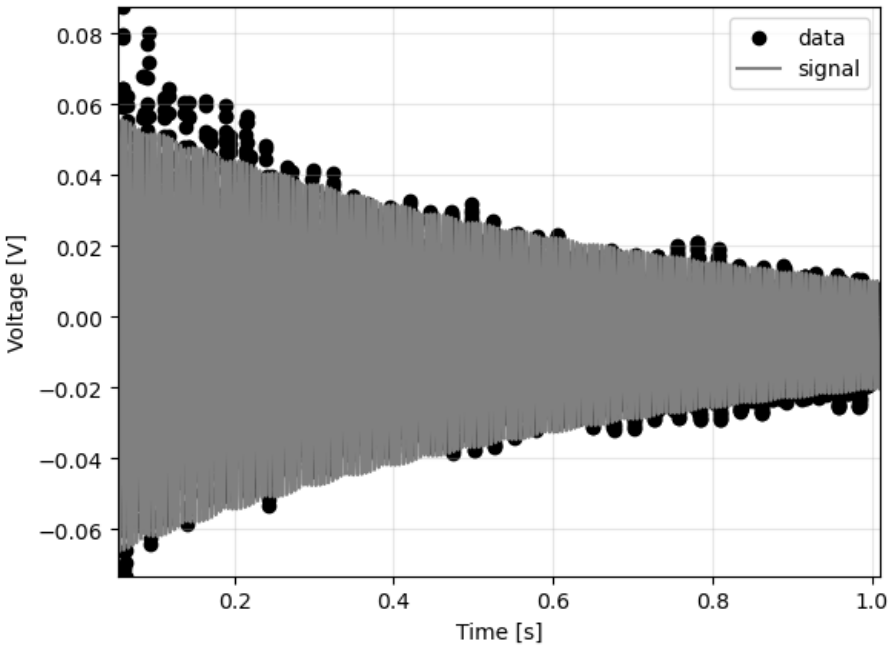

Figure 32: An equation fit to the rate of decay of the data.

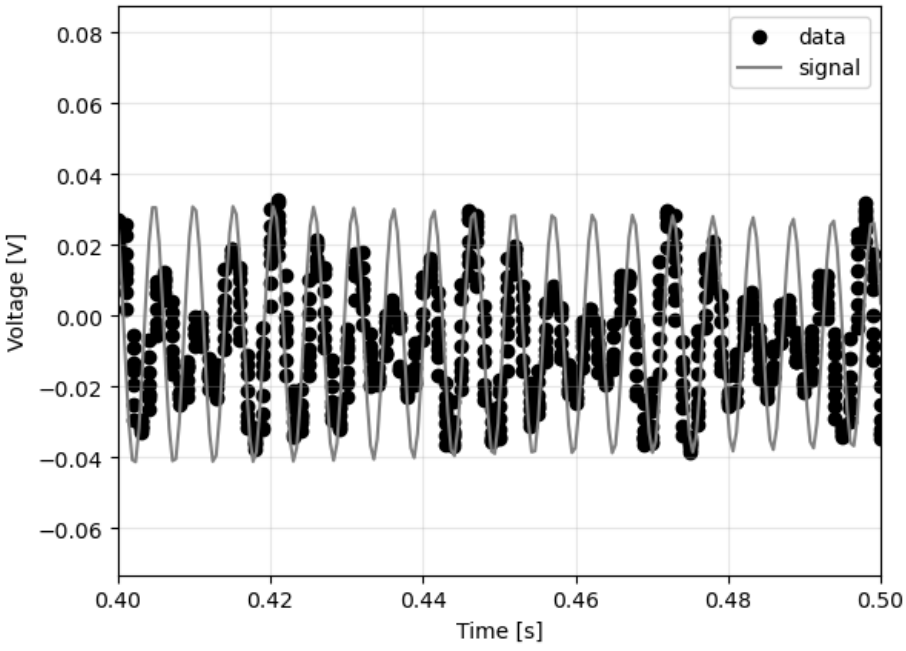

Figure 33: An equation fit to the frequency of the data.

A least squares fit was performed to get a sense of how the equation should look. After getting an idea for the range of the parameters, a Bayesian inference with Monte Carlo sampling was performed to obtain a probability distribution.

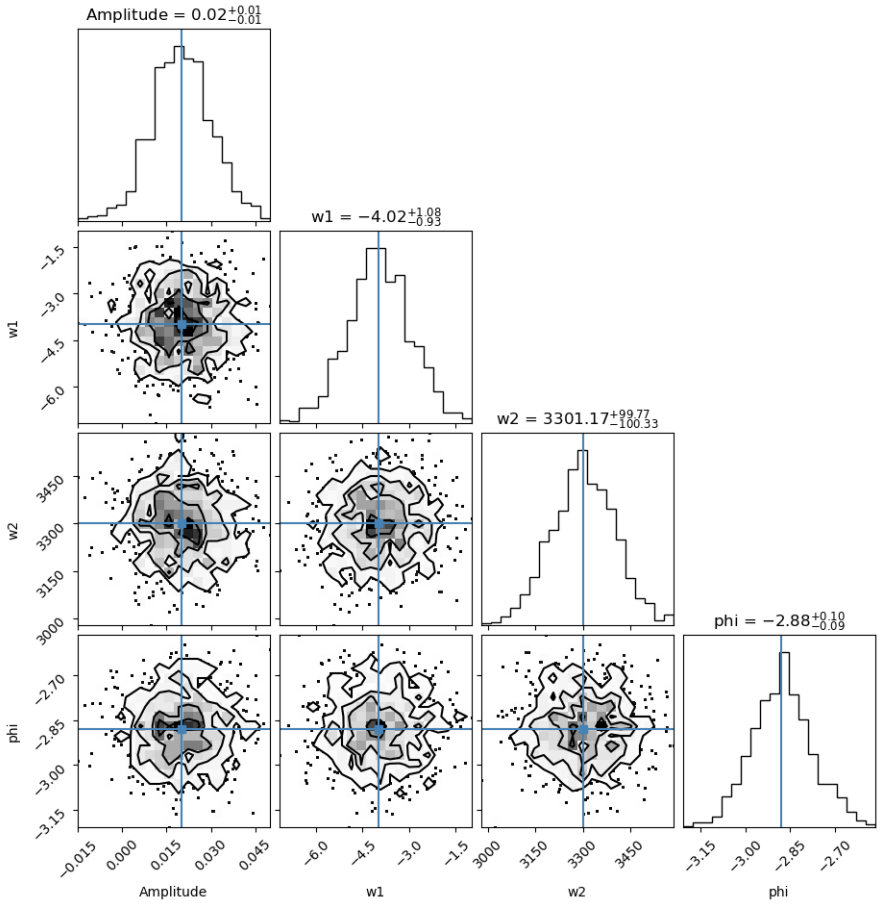

Figure 34: A corner plot showing the probability distribution.

Based on the equation $U(t) = U_0 e^{-\frac{\omega}{2Q}t}\cos\left(\omega t\sqrt{1-\frac{1}{4Q^2}}+\phi\right)$ where ω is the angular frequency, U_0 is the initial energy, ϕ is the phase shift, and Q is the quality factor,

$Q = \sqrt{\frac{(\frac{w_2}{w_1})^2+1}{4}} = 410 \pm 10.$

5 Conclusion

The question of how to determine the quality factor of an optically contacted silicon bond was approached by analyzing different cantilever geometries and dimensions in order to maximize the energy contribution of the bond. A rectangular cantilever with a 1.03 cm length, .5 mm width, and .1 mm height was selected. The optically bonded cantilever with the above dimensions still needs to be ordered and tested, but test data was obtained from an optical lever and analyzed using Bayesian inference. A quality factor of 410 ± 10 was measured, a value which is low but not unreasonable considering the test was done at room temperature with the vacuum off and with a well-used broken cantilever. For future work, it would be beneficial to estimate how much energy is lost through the clamp which holds the silicon cantilever.

References

[1] Wright, J. J. & Zissa, *D. E. OPTICAL CONTACTING FOR GRAVITY PROBE STAR TRACKER*. 14 (1984).

[2] Zawada, A., *Final Report: In-Vacuum Heat Switch*. 14.

[3] Douglas, R., *Aspects of hydroxide catalysis bonding of sapphire and silicon for use in future gravitational wave detectors*. (2017).

[4] Cesarini, E., Lorenzini, M., Cagnoli, G., & Piergiovanni, F. (2009). A gentle nodal suspension for measurements of the acoustic attenuation in materials. *2014 IEEE Metrology for Aerospace (MetroAeroSpace)*, 528-532.

[5] Nietzsche, S., Nawrodt, R., Zimmer, A., Thürk, M., Vodel, W., & amp; Seidel, P. (2006). Cryogenic Q-factor measurement of optical substrate materials. *Journal of Physics: Conference Series*, 32, 445–450. https://doi.org/10.1088/1742-6596/32/1/068

Acknowledgements

Thank you to Ian MacMillan for giving me the Pizza Cantilever COMSOL model. Thank you to Aaron Markowitz for helping me in the lab. Thank you Professor Rana Adhikari, Alan Weinstein, LIGO Caltech, and the National Science Foundation for providing guidance and making this research possible.